Journal of Computational Physics **152,** 1–31 (1999)
Article ID jcph.1999.6210, available online at http://www.idealibrary.com on IDEAL®

Numerical Simulation of Axisymmetric Viscous Flows by Means of a Particle Method

E. Rivoalen and S. Huberson

Laboratoire de Mécanique, 25 Rue Philippe Lebon, BP 540, 76058 Le Havre Cedex, France
E-mail: rivoalen@univ-lehavre.fr

Received September 3, 1996; revised December 28, 1998

A vortex particle method for the simulation of axisymmetric viscous flow is presented. The flow is assumed to be laminar and incompressible. The Navier–Stokes equations are expressed in an integral velocity-vorticity formulation. The inviscid scheme is based on Nitsche's method for axisymmetric vortex sheets. Meanwhile, two techniques are proposed for dealing with the viscous term. The first uses an integral Green's function method while the second is based on a diffusion velocity approach. Both are obtained by extension of existing methods for 2D flows. The problem of satisfying boundary conditions along the axis of symmetry is specifically addressed. The problem is solved by using cut-off functions that are derived from the Green's function of the axisymmetric diffusion equation. The scheme is applied to simulate the evolution of vortex rings at intermediate Reynolds number. The processes of entrainment and wake formation are evident in the calculations, as well as the extension of the support of vorticity due to viscous diffusion.

Key Words: particle method; diffusion; Navier–Stokes equations; vortex ring.

1. INTRODUCTION

In this paper, we present a numerical method for the simulation of unbounded axisymmetric viscous incompressible flows. Our method is based on a Lagrangian particle discretization. The advantage of the method is that it is well suited for the computation of slightly viscous, unbounded, or external flows. The introduction of viscous diffusion in vortex methods has been widely studied in the last 20 years. Many different techniques have been proposed and succesfully applied since the pioneering work by Chorin [6]. Basically, there are three main classes of algorithms: the first includes random-walk techniques, which are based on the analogy between Brownian motion and the effect of viscous diffusion on vortex particles. The second class [5, 7] of methods is based on an integral approximation of the diffusion operator. The third class of methods uses the so-called "diffusion velocity" approach. In this case the diffusion operator is, following algebraic manipulation,

0021-9991/99 $30.00

written as a convection operator and a single transport equation for the particles is solved [11, 9].

The extension of these methods to axisymmetric flows is faced with several difficulties, which require significant modification of the 2D algorithms on which the extension is based. Thus very few attempts have been made in that direction up to now, and only two methods have been significantly developed.

The first method is based on splitting of the (axisymmetric) diffusion operator into two parts: the first part consists of a Laplacian and is thus similar to the usual 2D diffusion operator. A random-walk method is used to simulate this term. The second part is accounted for in an explicit, "deterministic" fashion. This approach has been successfully applied to both external and internal flows; see, e.g., Martins and Ghoniem [13].

The second approach consists of introducing an axisymmetric flow assumption into a 3D method in order to reduce the computational cost. This has been done for vortex filaments [1, 17, 18], as well as particles. Although there is no account for viscous diffusion in these calculations, the extension of the integral method of [5, 7] is straightforward in that case and should be considered as a possible alternative. The use of the 3D diffusion velocity method [24] can also be envisaged.

In the present work, we will not consider the case of solid boundaries and will focus on the following three items:

- the extension of the 2D diffusion velocity and integral methods to the axisymmetric case;
- the treatment of external boundary conditions for unbounded flows;
- the treatment of boundary condition along the axis of symmetry.

The integral approximation for the diffusion operator is obtained using the Green's function of the axisymmetric diffusion equation and the conservative scheme of Choquin [5]. The diffusion velocity formulation is then obtained by an algebraic manipulation of the diffusion operator.

In the diffusion velocity method the external, far-field boundary conditions are automatically satisfied. On the other hand, the boundary conditions on the axis of symmetry provide a challenge. From this point of view, there is a basic difference between the 2D half plane problem and the axisymmetric meridian plane problem. The main difficulty lies in the computation of a smooth approximation of the velocity field close to the axis [20]. This problem is tackled by following an approach similar to the smoothing technique of Nitsche and Krasny [20]. Specifically, we first obtain a Green's function of the diffusion equation which satisfies the conditions on the axis of symmetry and use this Green's function in constructing a regularization kernel. The present situation differs from the vortex sheet study of Nitsche and Krasny since we are dealing with a distributed (viscous) vorticity field.

The scheme is used to compute the evolution of vortex rings at intermediate Reynolds number. Computed results are used to illustrate some of the properties of the diffusion velocity model and to check its accuracy by comparison with previously published solutions. The results also highlight the importance of proper treatment of conditions on the axis, especially when the vorticity support extends towards it.

2. THE PARTICLE METHOD FOR INVISCID AXISYMMETRIC FLOWS

If the azimuthal component of the velocity is zero, the vorticity field is organized as a set of circular vortex filaments or vortex rings. The governing equations can be written

as

$$\frac{\partial \xi}{\partial t} + u_r \frac{\partial \xi}{\partial r} + u_z \frac{\partial \xi}{\partial z} = 0 \tag{1}$$

$$\frac{\partial^2 \psi}{\partial z^2} + \frac{\partial^2 \psi}{\partial r^2} - \frac{1}{r}\frac{\partial \psi}{\partial r} = -r\omega, \tag{2}$$

where u_r and u_z are the radial and streamwise velocity components, respectively, ω is the vorticity, $\xi \equiv \omega/r$, and ψ is the streamfunction distribution, related to the velocity through

$$u_z = \frac{1}{r}\frac{\partial \psi}{\partial r} \tag{3}$$

$$u_r = -\frac{1}{r}\frac{\partial \psi}{\partial z}. \tag{4}$$

Equation (1) is a transport equation for ξ which is derived from the vorticity transport equation. For inviscid flows, it represents a pure convective equation similar to the vorticity transport equation for two-dimensional flows. Although ξ is no longer conserved for viscous flow, it underlies most of the existing vortex particle method for axisymmetric flows [13]. Since there is no dependence on the θ coordinate of the velocity and vorticity field, the computational domain reduces to an (r, z) plane for one selected value of θ (Fig. 1). In this representation of the flow, the vortex rings are described as a single point which is their intersection with the selected meridional plane. For inviscid flows, the ξ-equation can be easily interpreted thanks to Kelvin and Helmholtz theorems; since the circulation is constant along any vortex filament, any increase of the vortex ring radius must be accompanied by an increased vorticity.

An integral relation between the velocity field and the vorticity field can also be used. It is based on the the expression of the velocity at a given point (r, z) induced by the vortex ring with circulation Γ_0 located at the point (r_0, z_0),

$$\begin{aligned} u_z(r, z, r_0, z_0) &= \frac{\Gamma_0}{2\pi((r+r_0)^2 + (z-z_0)^2)^{1/2}} \left[\mathcal{K}(k) - \frac{(z-z_0)^2 + r^2 - r_0^2}{(r-r_0)^2 + (z-z_0)^2}\mathcal{E}(k)\right] \\ u_r(r, z, r_0, z_0) &= \frac{-\Gamma_0(z-z_0)}{2\pi r((r+r_0)^2 + (z-z_0)^2)^{1/2}} \left[\mathcal{K}(k) - \frac{r_0^2 + r^2 + (z-z_0)^2}{(r-r_0)^2 + (z-z_0)^2}\mathcal{E}(k)\right], \end{aligned} \tag{5}$$

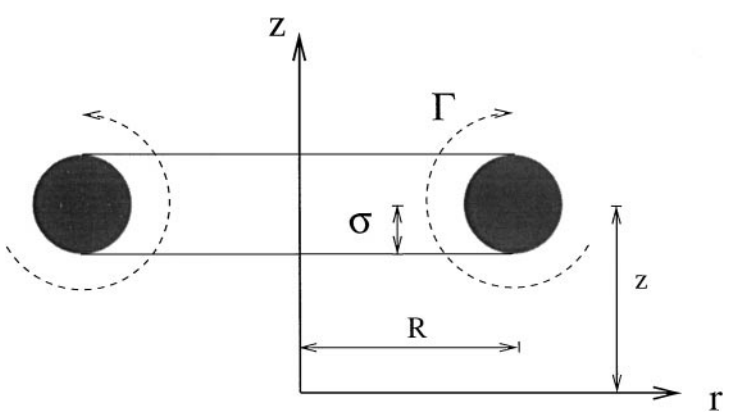

FIG. 1. Schematic sketch of the geometry for a circular vortex ring.

where $\mathcal{K}$ and $\mathcal{E}$ are first and second order elliptic functions, respectively, and

$$k \equiv \frac{4rr_0}{(r+r_0)^2+(z-z_0)^2} \tag{6}$$

is the argument.

It must be pointed out that these expressions are undefined at (r_0, z_0) where the velocity is singular. In the case of a pure two-dimensional flow, an easy way to remove the singularity, at least from a physical point of view, consists of considering that a point vortex actually represents a small blob of uniformly distributed vorticity. This technique can be readily transposed to axisymmetric flows although the result will be slightly different since the limit of the velocity at (r_0, z_0) is non-zero. The problem of determining the velocity of a vortex ring with a small core radius σ and a uniform vorticity distribution has been addressed by Lamb [15] who found the expression

$$\tilde{u}_z(r_0, z_0) \approx \frac{\Gamma_0}{4\pi r_0}\left\{\log\left(\frac{8r_0}{\sigma}\right) - \frac{1}{4}\right\}. \tag{7}$$

When using this expression, one must keep in mind that the point vortices are now considered as approximations of a vortex torus. For incompressible flows, the torus volume has to remain constant so that the core radius, σ, must be a function of the ring radius, r_0; we have

$$\sigma = \sqrt{\frac{\mathcal{T}}{2\pi^2 r_0}}, \tag{8}$$

where $\mathcal{T}$ is the volume of the torus. The numerical simulation of axisymmetric flows by means of particles can be reduced to computing the evolution of a finite number of vortex structures which are alternatively considered as vortex rings or vortex torus. The method based on the idea that particles are material elements has been shown by Raviart [23] and Cottet [8] to be second-order accurate for 2D flows.

Using this kind of discretization yields a singular velocity field at the center of each vortex ring. A desingularised approximation of the velocity induced by a set of vortex rings has been proposed by Nitsche [20]. The three-dimensional smoothing function used is the radially symmetric algebraic smoothing

$$\mathcal{H}(\beta) = \frac{3}{4\pi}\frac{1}{(\beta^2+1)^{5/2}}. \tag{9}$$

We also set

$$\mathcal{H}_\delta(\beta) = \frac{1}{\delta^3}\mathcal{H}\left(\frac{\beta}{\delta}\right), \tag{10}$$

where δ is the core radius. Thus, $\mathcal{H}_\delta$ is a 3D radially symmetric regular function of unit mass, whose limit as $\delta \to 0$ is the Dirac measure.

Inserting the smoothing parameter δ in the expression for the Stokes streamfunction ψ yields

$$\psi_\delta(r, z, r_0, z_0) = \frac{\Gamma_0}{2\pi}(\rho_1+\rho_2)(\mathcal{K}(\lambda) - \mathcal{E}(\lambda)), \tag{11}$$

where

$$\lambda = (\rho_2 - \rho_1)/(\rho_2 + \rho_1),$$
$$\rho_1^2 = (z - z_0)^2 + (r - r_0)^2 + \delta^2,$$

and

$$\rho_2^2 = (z - z_0)^2 + (r + r_0)^2 + \delta^2.$$

The velocity corresponding to the above streamfunction distribution is

$$u_{\delta r}(r, z, r_0, z_0) = -\frac{\Gamma_0}{r}\frac{\partial \psi_\delta}{\partial z}(r, z, r_0, z_0) \tag{12}$$

$$u_{\delta z}(r, z, r_0, z_0) = \frac{\Gamma_0}{r}\frac{\partial \psi_\delta}{\partial r}(r, z, r_0, z_0), \tag{13}$$

where

$$\frac{\partial \psi_\delta}{\partial z}(r, z, r_0, z_0) = (z - z_0)\left(\frac{1}{\rho_1}\frac{\partial \psi_\delta}{\partial \rho_1} + \frac{1}{\rho_2}\frac{\partial \psi_\delta}{\partial \rho_2}\right) \tag{14}$$

$$\frac{\partial \psi_\delta}{\partial r}(r, z, r_0, z_0) = \frac{r - r_0}{\rho_1}\frac{\partial \psi_\delta}{\partial \rho_1} + \frac{r + r_0}{\rho_2}\frac{\partial \psi_\delta}{\partial \rho_2} \tag{15}$$

and

$$\begin{aligned}\frac{\partial \psi_\delta}{\partial \rho_1} &= \frac{1}{2\pi}\left(\mathcal{K}(\lambda) - \frac{1}{2}\left(1 + \frac{\rho_2}{\rho_1}\right)\mathcal{E}(\lambda)\right),\\ \frac{\partial \psi_\delta}{\partial \rho_2} &= \frac{1}{2\pi}\left(\mathcal{K}(\lambda) - \frac{1}{2}\left(1 + \frac{\rho_1}{\rho_2}\right)\mathcal{E}(\lambda)\right).\end{aligned} \tag{16}$$

On the axis, $r = 0$, these expressions have the finite limits

$$u_{\delta r}(0, z, r_0, z_0) = \frac{\Gamma_0}{2}\frac{r_0^2}{\left((z - z_0)^2 + r_0^2 + \delta^2\right)^{3/2}}, \qquad u_{\delta z}(0, z, r_0, z_0) = 0. \tag{17}$$

This leads to a set of ordinary differential equations for the location of the particles which will be defined by their two coordinates (r_i, z_i) and their circulation Γ_i,

$$\begin{aligned}\frac{d\Gamma_i}{dt} &= 0\\ \frac{dr_i}{dt} &= \sum_j u_{\delta r}(r_i, z_i, r_j, z_j)\\ \frac{dz_i}{dt} &= \sum_j u_{\delta z}(r_i, z_i, r_j, z_j).\end{aligned} \tag{18}$$

3. THE DIFFUSION ALGORITHMS

3.1. *Introduction*

In this section, we are interested in the numerical simulation of the viscous diffusion of vorticity. In order to simplify the presentation, we consider a simple diffusion equation,

which can be regarded as a fractional step resulting from the splitting of the problem into a convective part

$$\frac{\partial}{\partial t}\left(\frac{\omega}{r}\right) + \boldsymbol{\nabla}\cdot\mathbf{U}\left(\frac{\omega}{r}\right) = 0 \tag{19}$$

and a diffusion part

$$\frac{\partial \omega}{\partial t} = \nu\left(\frac{\partial^2\omega}{\partial r^2} + \frac{\partial^2\omega}{\partial z^2} - \frac{\omega}{r^2} + \frac{1}{r}\frac{\partial\omega}{\partial r}\right). \tag{20}$$

(We shall not actually use such a splitting in the present work.) Thus we only focus on the solution of Eq. (20). This is a diffusion equation for which a boundary condition is required all around the computational domain. Because the particle method is able to deal with unbounded domains, we only consider unbounded flow and that the computational domain is the half-plane $r > 0$. There are boundary conditions at infinity which are automatically satisfied as long as the particles remain confined to a bounded part of this plane. Some attention has to be paid to the boundary conditions along the axis. From the regularity of the velocity field on the axis,

$$\begin{aligned} u_r &= 0 \\ \frac{\partial u_z}{\partial r} &= 0, \end{aligned} \tag{21}$$

the following condition is obtained for the vorticity:

$$\omega = \frac{\partial u_r}{\partial z} - \frac{\partial u_z}{\partial r} = 0. \tag{22}$$

The z axis is a material line where the vorticity flux across this line is non-zero. The leak of circulation is given directly using the relation

$$\frac{d\Gamma}{dt} = -\nu\int_{-\infty}^{+\infty}\left(\frac{\partial\omega}{\partial r} + \frac{\omega}{r}\right)\bigg|_{r=0} dz \tag{23}$$

which in turn has no obvious reason to be zero in the discrete formulation. This result is a problem when solving the vorticity transport equation since the axis is at the same time a region where the quantity ξ is difficult to compute, due to the smallness or nullity of r, and a region where there may be an apparent vorticity production. This production is said to be "apparent" because it can only be an artifact of the numerical formulation.

3.2. *The Strength Exchange Model*

A first way to solve the diffusion problem is to make use of the explicit solution arising from heat transfer theory. The main difference between our approach and the corresponding one in the thermal diffusion problem is that our boundary condition along the axis is meaningless from a thermal point of view [3]. An easy way to obtain the solution with the right boundary condition is to extend the problem to the whole space, that is, to compute the solution even in the $r < 0$ part of the space, and to use the antisymmetric initial condition. The problem to be solved consists of the diffusion equation (20), with initial conditions.

We use separation of variables in order to reduce our problem to an ordinary differential equation. For a circular vortex ring of circulation Γ_0 that is concentrated at point (r_0, z_0) at time $t = 0$, we asume that the solution can be expressed as

$$\omega(r, z, t) = \frac{2\pi r_o \Gamma_o}{(4\pi t\nu)^{3/2}} \exp\left(-\frac{r^2 + r_o^2 + (z - z_o)^2}{4t\nu}\right) \mathcal{F}(r, t) \tag{24}$$

and find that the function $\mathcal{F}(r, t)$ is the modified Bessel function of first order, $\mathcal{I}_1$. We have now the explicit solution of the diffusion problem of an axisymmetric flow with inital condition specified before,

$$\omega(r, z, t) = \frac{2\pi r_o \Gamma_o}{(4\pi t\nu)^{3/2}} \exp\left(-\frac{(r - r_o)^2 + (z - z_o)^2}{4t\nu}\right) \exp\left(-\frac{r r_o}{2t\nu}\right) \mathcal{I}_1\left(\frac{r r_o}{2t\nu}\right). \tag{25}$$

This solution is used to solve the vorticity diffusion equation with the formulation used in [5]. The extension of the integral formulation of the diffusion operator is obtained by replacing the 2D Green function by (25),

$$\begin{aligned}\omega(r, z, t + \Delta t) = \int_S \frac{2\pi r_o \omega(r_o, z_o, t)}{(4\pi \Delta t\nu)^{3/2}} \exp\left(-\frac{(r - r_o)^2 + (z - z_o)^2}{4\Delta t\nu}\right) \\ \times \exp\left(-\frac{r r_o}{2\Delta t\nu}\right) \mathcal{I}_1\left(\frac{r r_o}{2\Delta t\nu}\right) dr_o\, dz_o.\end{aligned} \tag{26}$$

S is the support of ω in the half plane (r, z). The use of this solution within a particle method requires some care in order to preserve the global conservation of the vorticity (see the Appendix). In particular the flux of vorticity along the z axis should be taken into account by using Eq. (23).

The discrete form of Eq. (26) is readily obtained following the analysis proposed in [5]; we have

$$\begin{aligned}\Gamma_i(t + \Delta t) = \Gamma_i(t)\left(1 - \exp\left(-\frac{r_i^2}{4\Delta t\nu}\right)\right) + \sum_{j \neq i} (r_j \Gamma_j \mathcal{S}_i - r_i \Gamma_i \mathcal{S}_j) \frac{2\pi}{(4\pi \Delta t\nu)^{3/2}} \\ \times \exp\left(-\frac{(r_i - r_j)^2 + (z_i - z_j)^2}{4\Delta t\nu}\right) \exp\left(-\frac{r_i r_j}{2\Delta t\nu}\right) \mathcal{I}_1\left(\frac{r_i r_j}{2\Delta t\nu}\right).\end{aligned} \tag{27}$$

The first term on the right hand side of Eq. (27) corresponds to the circulation of particle i after a small amount of vorticty has been dissipated on the axis according to Eq. (23). The second term represents the exchange of circulation between particles and it is straightforward to verify that this part conserves the total circulation provided the particles cover the whole half plane. Also notice that the use of a symmetric cut off function would have led to the necessity of having particles covering the whole plane, even for negative r. This sheds light on the problem which can be encountered when satisfying the boundary condition along the axis.

3.3. *The Diffusion Velocity Model*

3.3.1. Convective formulation of the diffusion equation. Convective analogues for diffusion have been extensively used for building numerical algorithms. The method consists

of a transformation of the convection-diffusion equation into a pure convection equation,

$$\frac{\partial \xi}{\partial t} + \nabla \cdot (\mathbf{U} + \mathbf{U}_v)\xi = 0. \tag{28}$$

It is not obvious whether this transformation is always possible. The problem is that the resulting equation must be equivalent to the initial one. This can be easily achieved for 2D flows and has been demonstrated by many authors [9, 11]. In the case of axisymmetric flows, additional algebraic manipulation is required. At first, we write the right hand side of Eq. (20) in a divergence form. We have

$$\frac{\partial^2 \xi}{\partial r^2} + \frac{\partial^2 \xi}{\partial z^2} + \frac{3}{r}\frac{\partial \xi}{\partial r} = \nabla \cdot (r^{-2}\nabla(r^2\xi)). \tag{29}$$

The convective form in (28) is then readily obtained using

$$\mathbf{U}_v = -\nu \frac{(\nabla(r^2\xi))}{r^2\xi}. \tag{30}$$

Considering now Eqs. (28) and (30), it can be observed that the extension of the vorticity support is automatically accounted for by the particles since the diffusion velocity will be large in the external region, due to the smallness of the vorticity. This will obviously lead to an increased inter-particle distance and the phenomenon can be interpreted as roughly analogous to the use of a coarser mesh in the outer region for grid methods. The use of the diffusion velocity will lead to the definition of a pseudo "constant weight" method in the sense that this property is only true for ξ and during the integration of Eq. (28).

3.3.2. Computation of the diffusion velocity. The problem to be addressed in this section is that of the particle discretization of Eq. (30). First, we can write this equation in term of the vorticity ω; we have

$$\mathbf{U}_v = (u_{vr}, u_{vz}) = -\frac{\nu}{\omega}\left(\frac{\partial \omega}{\partial r} + \frac{\omega}{r}, \frac{\partial \omega}{\partial z}\right). \tag{31}$$

Thus it is necessary to define a continuous vorticity field in the plane (r, z) as well as its derivatives with respect to r and z. Once again, the technique is based on what is done for two- and three-dimensional particle methods. We start with the approximate identity,

$$\boldsymbol{\omega}_\varepsilon(\mathbf{x}) = \int_V \mathcal{F}_\varepsilon(\mathbf{x} - \mathbf{x}')\boldsymbol{\omega}(\mathbf{x}')\, dv(\mathbf{x}'), \tag{32}$$

where $\mathcal{F}_\varepsilon$ is a smoothing function having the same properties of $\mathcal{H}_\delta$ (see Eq. (10)).

The axisymmetric configuration makes it convenient to use a cylindrical coordinate system (e_r, e_θ, e_z). In our case $\boldsymbol{\omega} = \omega \cdot e_\theta$ and the vorticity is computed in the half plane and $r > 0$. In this coordinate system Eq. (32) takes the form

$$\omega_\varepsilon(r, z) = \int_S \omega(r', z') \int_0^{2\pi} \mathcal{F}_\varepsilon(\rho)\cos(\theta)\, d\theta r'\, dr'\, dz', \tag{33}$$

where S is the semi-infinite meridional plane and ρ is the distance between a point in the half plane (r, z) and a point in V,

$$\rho^2 = r^2 + r'^2 + (z - z')^2 - 2rr'\cos(\theta). \tag{34}$$

The possibility to derive an analytical solution for the integral is directly related to the choice for $\mathcal{F}_\varepsilon$. We illustrate the method by using the second-order, three-dimensional Gaussian smoothing

$$\mathcal{F}_\varepsilon(\mathbf{x}-\mathbf{x}') = \frac{1}{(\pi\varepsilon^2)^{3/2}} \exp\left(-\frac{|\mathbf{x}-\mathbf{x}'|^2}{\varepsilon^2}\right). \tag{35}$$

We then substitute Eq. (35) into Eq. (33) and isolate all the terms which do not depend on θ. We have

$$\omega_\varepsilon(r,z) = \int_S \frac{\omega(r',z')}{(\pi\varepsilon^2)^{3/2}} \exp[-(r^2+r'^2+(z-z')^2)/\varepsilon^2]\mathcal{J}(r,r')r'\,dr'\,dz', \tag{36}$$

where

$$\mathcal{J}(r,r') = \int_0^{2\pi} \cos(\theta)\exp(2\cos(\theta)rr'/\varepsilon^2)\,d\theta. \tag{37}$$

The result of the last integral is

$$\mathcal{J}(r,r') = 2\pi I_1(2rr'/\varepsilon^2). \tag{38}$$

Thus Eq. (33) becomes

$$\omega_\varepsilon(r,z) = \int_S \frac{\omega(r',z')}{(\pi\varepsilon^2)^{3/2}} \exp[-(r^2+r'^2+(z-z')^2)/\varepsilon^2]I_1(2rr'/\varepsilon^2)2\pi r'\,dr'\,dz'. \tag{39}$$

Discretizing the surface S using particles with $\Gamma = \omega(r',z')\,dr'\,dz'$, we obtain a discrete form for the local vorticity

$$\omega_\varepsilon(r,z) = \sum_{i=1}^{n} \frac{2\pi\Gamma_i r_i}{(\pi\varepsilon^2)^{3/2}} \exp\left[-\left(r^2+r_i^2+(z-z_i)^2\right)/\varepsilon^2\right] I_1\left(2rr_i/\varepsilon^2\right) \tag{40}$$

for which we deduce the final form of the Gaussian smoothing function for axisymmetric flow

$$\mathcal{G}_\varepsilon(r,z,r_i,z_i) = \frac{2r_i}{(\sqrt{\pi}\varepsilon^3)} \exp\left(-\frac{(z_i-z)^2+(r_i-r)^2}{\varepsilon^2}\right) \exp\left(-\frac{2r_i r}{\varepsilon^2}\right)\mathcal{I}_1\left(\frac{2r_i r}{\varepsilon^2}\right). \tag{41}$$

Then we get

$$\omega_\varepsilon(r,z) = \sum_{i=1}^{n} \Gamma_i \cdot \mathcal{G}_\varepsilon(r,z,r_i,z_i). \tag{42}$$

The function $\mathcal{G}_\varepsilon$ is the product of the one-dimensional Gaussian smoothing function for the z coordinate and the one-dimensional axisymmetrical Gaussian function for the z coordinate. Then

$$\mathcal{G}_\varepsilon(r,z,r_0,z_0) = \mathcal{G}_{z\varepsilon}(z,z_0)\mathcal{G}_{r\varepsilon}(r,r_0) \tag{43}$$

with

$$\mathcal{G}_{z\varepsilon}(z, z_0) = \frac{1}{\sqrt{\pi\varepsilon^2}} \exp\left(-\frac{(z_0 - z)^2}{\varepsilon^2}\right) \tag{44}$$

and

$$\mathcal{G}_{r\varepsilon}(r, r_0) = \frac{2r_0}{\varepsilon^2} \exp\left(-\frac{(r_0 - r)^2}{\varepsilon^2}\right) \exp\left(-\frac{2r_0 r}{\varepsilon^2}\right) \mathcal{I}_1\left(\frac{2r_0 r}{\varepsilon^2}\right). \tag{45}$$

The use of non-symmetric functions for the r component (45) does not respect the usual moment conditions for the core functions used in particle method [2]. Using the series development for $\mathcal{G}_{r\varepsilon}$ [16] it is straightforward to verify that

$$\int_S \mathcal{G}_{r\varepsilon}(r, r_0) r^2 \, dr = r_0^2 \tag{46}$$

irrespective of the value for ε. Then if we consider a vortex ring Γ_0, the total impulse I associated with this ring is preserved,

$$\mathrm{I} = \pi \int_S \omega_\varepsilon r^2 \, dr \, dz = \pi \Gamma_0 r_0^2. \tag{47}$$

Using the same technique we can also verify that

$$\int_S \mathcal{G}_{r\varepsilon}(r, r_0) \, dr = 1 - \exp\left(-\frac{r_0^2}{\varepsilon^2}\right). \tag{48}$$

There is no existing mathematical analysis of this problem so it has been conjectured that the construction of this function by using the solution of the diffusion equation should be second-order, as it is the case for the Gaussian function in 2D.

Note that the smoothing function (9) used to desingularize the velocity differs from the Gaussian smoothing function used to estimate the vorticity field (35). This is purely formal because both ε and δ are smoothing parameters. The $\mathcal{G}_\varepsilon$ function has been derived in order to satisfy the boundary conditions, that is, zero vorticity on the axis.

Thus, there is no obvious mathematical relation between δ and ε; it has been found from numerical experiments that $\varepsilon = 2\delta$ provides comparable self-induced velocities. The selection of two different functions has been made only in order to simplify the computational work. The gradient of ω is obtained by a direct differentiation of Eq. (42). Thus, we get the expressions

$$\begin{aligned}\frac{\partial \omega_\varepsilon}{\partial r} + \frac{\omega_\varepsilon}{r} = &\sum_{i=1}^{n} \frac{-4 r r_i \Gamma_i}{(\sqrt{\pi}\varepsilon^5)} \exp\left(-\frac{(z_i - z)^2 + (r_i - r)^2}{\varepsilon^2}\right) \exp\left(-\frac{2 r_i r}{\varepsilon^2}\right) \mathcal{I}_1\left(\frac{2 r_i r}{\varepsilon^2}\right) \\ &+ \sum_{i=1}^{n} \frac{4 r_i^2 \Gamma_i}{(\sqrt{\pi}\varepsilon^5)} \exp\left(-\frac{(z_i - z)^2 + (r_i - r)^2}{\varepsilon^2}\right) \exp\left(-\frac{2 r_i r}{\varepsilon^2}\right) \mathcal{I}_0\left(\frac{2 r_i r}{\varepsilon^2}\right)\end{aligned} \tag{49}$$

$$\frac{\partial \omega_\varepsilon}{\partial z} = \sum_{i=1}^{n} \frac{4 r_i (z_i - z) \Gamma_i}{(\sqrt{\pi}\varepsilon^5)} \exp\left(-\frac{(z_i - z)^2 + (r_i - r)^2}{\varepsilon^2}\right) \exp\left(-\frac{2 r_i r}{\varepsilon^2}\right) \mathcal{I}_1\left(\frac{2 r_i r}{\varepsilon^2}\right) \tag{50}$$

which are then used in the evaluation of diffusion velocity.

We will present the complete algorithm with the diffusion velocity method of Subsection 3.3 because it leads to a somewhat simpler formulation. Putting together the equations which have been established in Section 2 and Subsections 3.3.2 and 4.2, we obtain a complete model for the Navier–Stokes problem:

$$\begin{aligned}
\frac{d\Gamma_i}{dt} &= -\nu \frac{4r_i^2\Gamma_i}{\varepsilon^4} \exp\left(-\frac{r_i^2}{\varepsilon^2}\right) \\
\frac{dr_i}{dt} &= \sum_j u_{\delta r}(r_i, z_i, r_j, z_j) + u_{vr}(r_i, z_i, r_j, z_j) \\
\frac{dz_i}{dt} &= \sum_j u_{\delta z}(r_i, z_i, r_j, z_j) + u_{vz}(r_i, z_i, r_j, z_j).
\end{aligned} \tag{51}$$

The time integration scheme which will be used in the calculations is a 4th order accurate Runge–Kutta scheme.

4. DISCRETIZATION OF THE INITIAL CONDITION

4.1. *Initial Conditions*

In Section 5 the numerical scheme is applied to simulate viscous vortex rings. To initialize the computations, particles are distributed inside a torus section of radius r_v on N_c concentric circles and with one particle at the center of the section (Fig. 2). The distance between two neighboring circles is $\Delta y = r_v/(N_c + 0.5)$ and the radius of the circle represented by the particle at the center is $\Delta y/2$. N_p is the number of particles on the first circle and it becomes $2N_p$ for the second circle and iN_p for the ith circle. Then the initial total number of particles is $N = N_p N_c(N_c+1)/2 + 1$. The angle between two successive particles placed on the same circle i is $\Delta\varphi_i = 2\pi/iN_p$. The same process of discretization is used by Knio

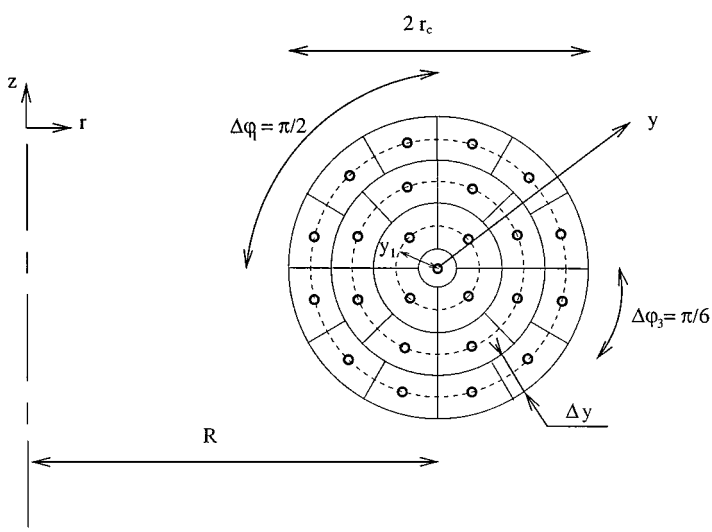

FIG. 2. Initial positions of particles before merging and splitting algorithm in the cross section of the ring.

TABLE I
Discretization Parameters for Axisymmetric and Norbury Sections

Grid	Section	$(r_v/R, N_p, N_c)$	Total number of particles	Case 1		Case 2		Case 3	
				ε_0/R	N	ε_0/R	N	ε_0/R	N
1	Axisym.	(0.65, 4, 50)	5101	0.015	3401	0.025	901	0.03	460
2	Axisym.	(0.06, 2, 30)	931	0.004	344	0.006	162	0.008	84
3	Norbury	(0.5, 4, 50)	5101	0.01	4249	0.015	1697	0.02	846

and Ghoniem [14] to initialize the core section of 3D vortex ring. The initial geometrical properties of particles are the position (r_i, z_i), the surface $S_i = y_i \Delta y \Delta\varphi_i$, and then the volume $\mathcal{T}_i = 2\pi r_i S_i$. An equivalent core radius σ_i is calculated on each particle:

$$\sigma_i = \sqrt{\frac{\mathcal{T}_i}{2\pi^2 r_i}}.$$

The same technique is used to initialize a Norbury section [22] which defines a numerical family of steadily translating inviscid vortex rings. In Table I some initial conditions for the axisymmetric core and Norbury core are given. Starting from this initial configuration we apply a merging and splitting algorithm for initial different values of (r_v, N_p, N_c) and for different values for ε_0. This technique which is described in the next section is necessary to ensure that the density of particles in all the sections is the same.

In Figs. 3 and 4, a set of nested particle distributions is presented. They are obtained by applying the merging/splitting algorithm with increasing ε_0.

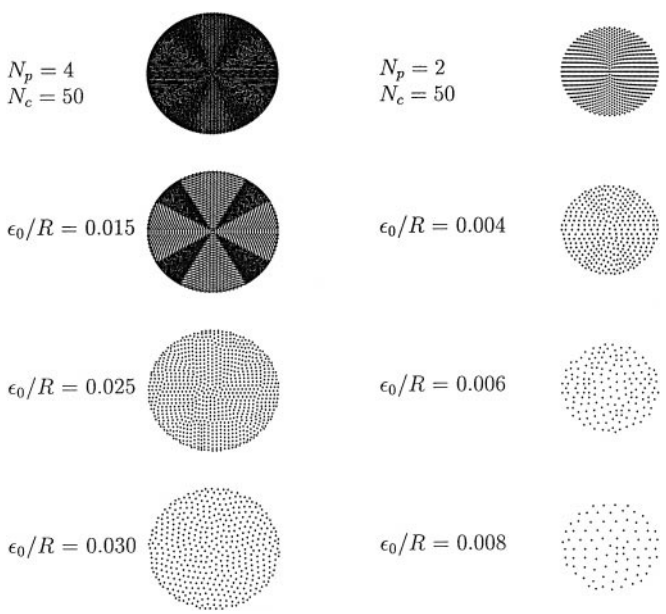

FIG. 3. Effect of the merging algorithm on two axisymmetric sections for different values of ε_0.

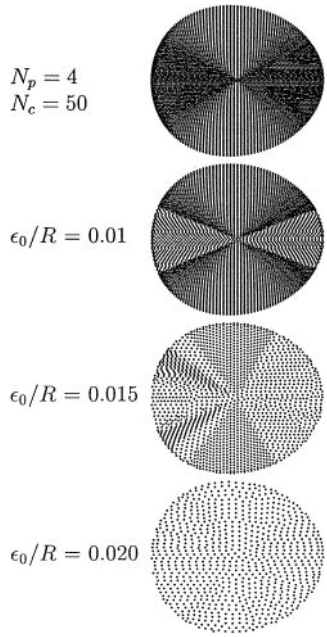

FIG. 4. Effect of the merging algorithm on a Norbury section for three different values of ε_0.

4.2. *Re-griding Procedure*

The splitting-merging procedure has been designed in order to satisfy the conservation for the total circulation Γ and the total impulse I [15] during the re-griding procedure,

$$\begin{aligned} \Gamma &= \int_S \omega \, dr \, dz \\ \mathrm{I} &= \pi \int_S \omega r^2 \, dr \, dz. \end{aligned} \tag{52}$$

The geometrical position of the center of particles is defined by the center of vorticity,

$$\tilde{r}^2 = \frac{\int_S \omega r^2 \, dr \, dz}{\int_S \omega \, dr \, dz}, \qquad \tilde{z} = \frac{\int_S \omega r^2 z \, dr \, dz}{\int_S \omega r^2 \, dr \, dz}. \tag{53}$$

The discrete coordinates $(\tilde{r}, \tilde{z})$ are expressed in term of the coordinate of the particles representing the equivalent vortex system,

$$\tilde{r} = \sqrt{\frac{\sum_j r_j^2 \Gamma_j}{\sum_j \Gamma_j}}, \qquad \tilde{z} = \frac{\sum_j r_j^2 z_j \Gamma_j}{\sum_j r_j^2 \Gamma_j} \tag{54}$$

$$\tilde{\Gamma} = \sum_j \Gamma_j. \tag{55}$$

In the calculations, a particle is split whenever $\sigma_i > \varepsilon_0$. The procedure is applied for all particles in the set $\mathcal{D}$,

$$\mathcal{D} = \{M_i(r_i, z_i) \quad / \quad \sigma_i > \varepsilon_0\}, \tag{56}$$

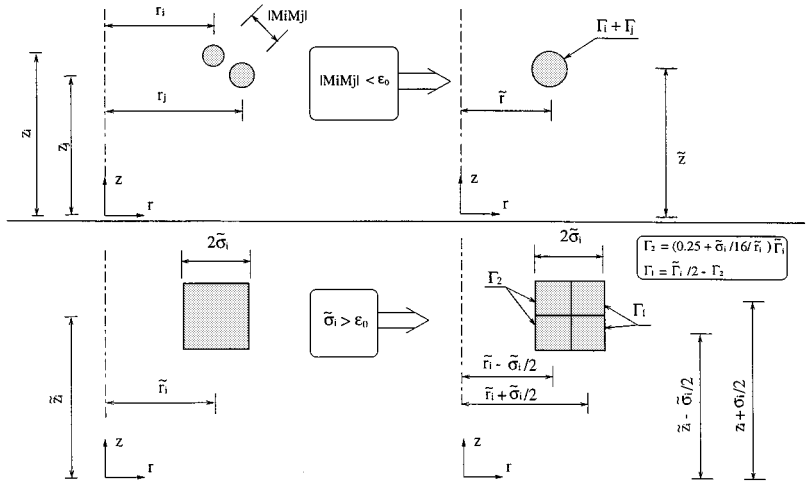

FIG. 5. Merging (top) and splitting (bottom) of vortex particles.

where $\mathcal{D}$ is the set of particles M_i for which the core radius σ_i is greater than the size ε_0. If $M_i \in \mathcal{D}$, it is split into four new particles.

Conversely, the merging of two particles M_i and M_j into one particle is performed whenever distance $|M_i M_j|$ feels below ε_0. The element pairs undergoing merging belong to the set

$$\mathcal{A} = \{(M_i, M_j) \quad / \quad |M_i M_j| < \varepsilon_0\}. \tag{57}$$

If this distance is large enough, we check that none of the condition defining $\mathcal{D}$ is fulfilled by the two particles. This is exactly the object of the condition. The two sets $\mathcal{D}$ and $\mathcal{A}$ are non-overlapping. This can be easily checked by considering once again the fluid volume represented by each particle. Once one or two particles are found that belong to one of the two sets $\mathcal{D}$ and $\mathcal{A}$, the splitting and merging operations are activated.

Applying relation (55) to our problem will lead to the following result: in case of merging of two particles, $(\tilde{r}_i, \tilde{z}_i, \tilde{\Gamma}_i, \tilde{\mathcal{T}}_i)$ have to be computed whereas $(r_j, z_j, \Gamma_j, \mathcal{T}_j)_{j=1,4}$ have to be computed in a splitting step (Fig. 5). Each particle has the same core radius and the circulation is calculated to preserve the total circulation and the total impulse. The two procedures are performed simultaneously. Then, the merging and splitting criteria are checked once again for all the particles and the process repeated until the sets $\mathcal{D}$ and $\mathcal{A}$ are empty. Finally we have defined a geometrical and fixed parameter ε_0 which is a representation of the optimal value for the distance between two particles and for one particle core radius. It is usual in vortex methods to choose the smoothing parameter δ or ε greater than the averaged distance between two particles ε_0 in order to ensure the quality of the approximated velocity field (57) and (56).

5. RESULTS

5.1. *Validation Test*

We analyse the effect of time step Δt and discretization parameter ε_0 on the temporal evolution of two different initial distributions of vorticity on the ring core:

• The initial vorticity distribution in the (r, z) plane is a vortex ring with Gaussian core section:

$$\begin{cases} \omega = \frac{\Gamma_0}{\pi\sigma_0^2} \exp -\left(\frac{y}{\sigma_0}\right)^2 & \text{with} \\ y^2 = (z_0 - z)^2 + (r_0 - r)^2. \end{cases} \tag{58}$$

In the thin tube approximation the vortex ring translation velocity is given by the asymptotic expression

$$U_{zc} = \frac{dz_c}{dt} = \frac{\Gamma_0}{4\pi r_0}\left\{\log\left(\frac{8r_0}{\sigma_0}\right) - C\right\}, \tag{59}$$

where C depends of vorticity distribution inside the core. For a Gaussian distribution $C = 0.558$, Eq. (59) is valid as long as the core radius σ_0 remains small compared to the tore radius r_0. The core radius is fixed here to $\sigma_0/r_0 = 0.03$ in all tests and the diffusion process is not activated. In Fig. 6 the effect of Δt is analyzed. The velocity of the vorticity centroid $U(t) = \frac{d\tilde{z}}{dt}$ where $\tilde{z}$ is defined in Eq. (53) is compared to the asymptotic prediction $U_{th} \equiv U_{zc}$. The velocity oscillates a little in time and decreases when the time step $\Delta t\Gamma/R^2$ is biger than 0.004. The $\tilde{r}$ component of vorticity centroid (Eq. (53)) should remain constant here. $\tilde{r}^2$ is the ratio between the total impulse and the total circulation. The trajectory of the vorticity centroid is represented in Fig. 7. The particle method preserves the total circulation. However, when the time step is too large (>0.004 here) Fig. 7 shows that the impulse is not preserved because the r component increases when the time step increases. The time step is fixed now. In Fig. 8 the number of particles in the section is tested by changing the parameter ε_0. To have a good representation of the section, the number of particles should

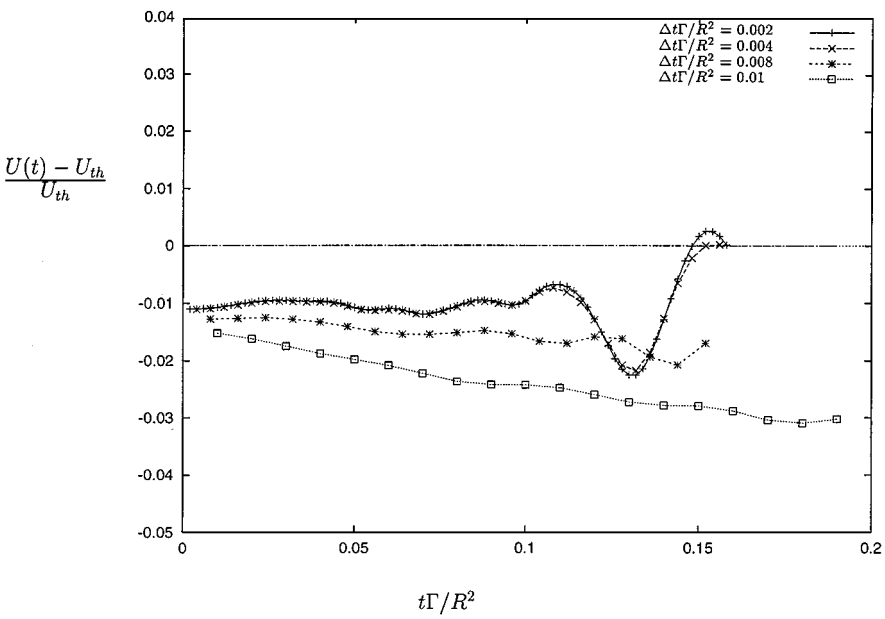

FIG. 6. Evolution of the core self induced velocity for different values of the time step $\Delta t\Gamma/R^2$. The initial repartition of vorticity in the section is Gaussian. The initial distribution of the particle is $(r_v/R, N_p, N_c) = (0.08, 4, 50)$ and $\varepsilon_0/R = 0.005$, $\delta/R = 0.005$.

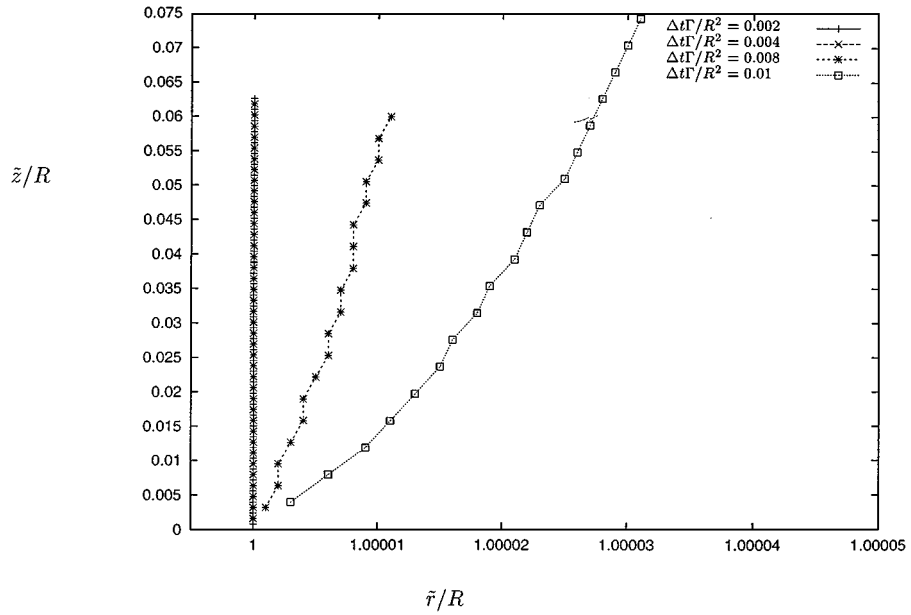

FIG. 7. Trajectory of the vorticity centroid for different values of the time step $\Delta t\Gamma/R^2$, $\delta/R = 0.005$.

be greater than 300 and in that case there is no significant difference between computed results of self induced velocity.

- Linear distribution of vorticity on Norbury section:

$$\frac{\omega}{r} = 1. \tag{60}$$

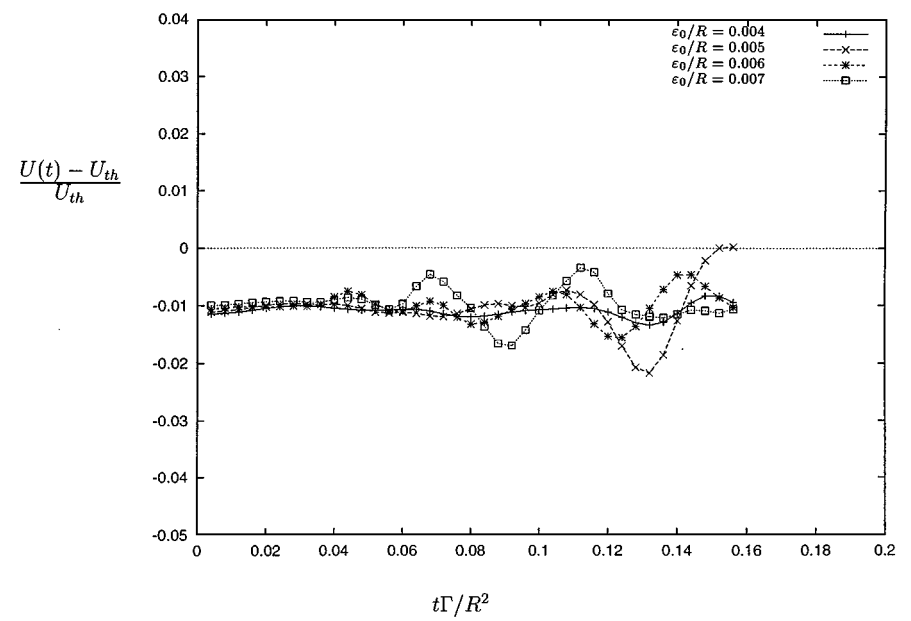

FIG. 8. Velocity of the vorticity centroid for different values of the size parameter ε_0/R. The time step is $\Delta t\Gamma/R^2 = 0.004$ and $\delta/R = 0.005$.

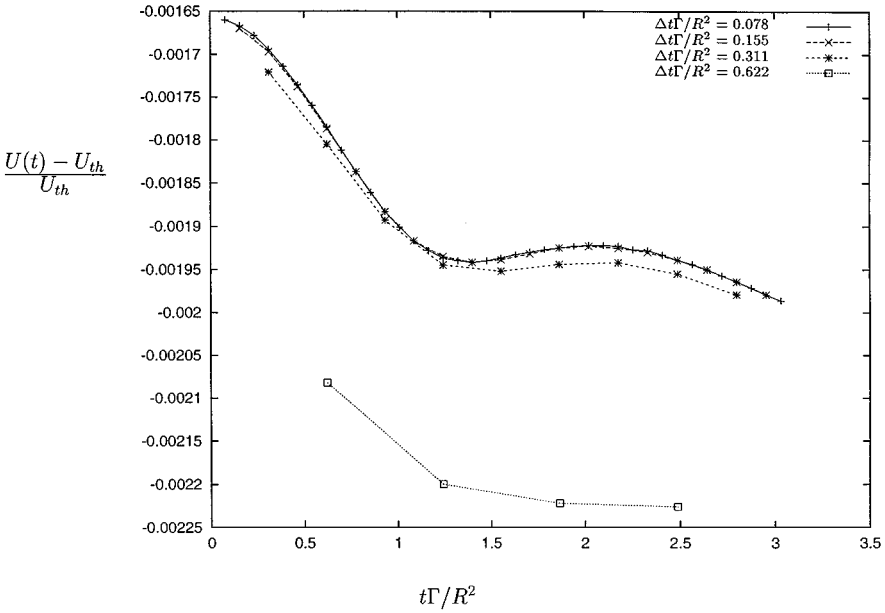

FIG. 9. Velocity of the vorticity centroid of a Norbury section for different values of the time step $\Delta t\Gamma/R^2$, $\delta/R = 0.03$, and $\varepsilon_0/R = 0.022$.

For different values of the time step the temporal evolution of the self-induced velocity is compared to the theoretical prediction in [22]. Figure 9 shows that when the time step is small enough ($\Delta t\Gamma/R^2 < 0.200$) the two results are very close. For too large time step the velocity is not large enough and like for a gaussian section when we plot the trajectory of the ring on Fig. 10 we can deduce that the impulse increases.

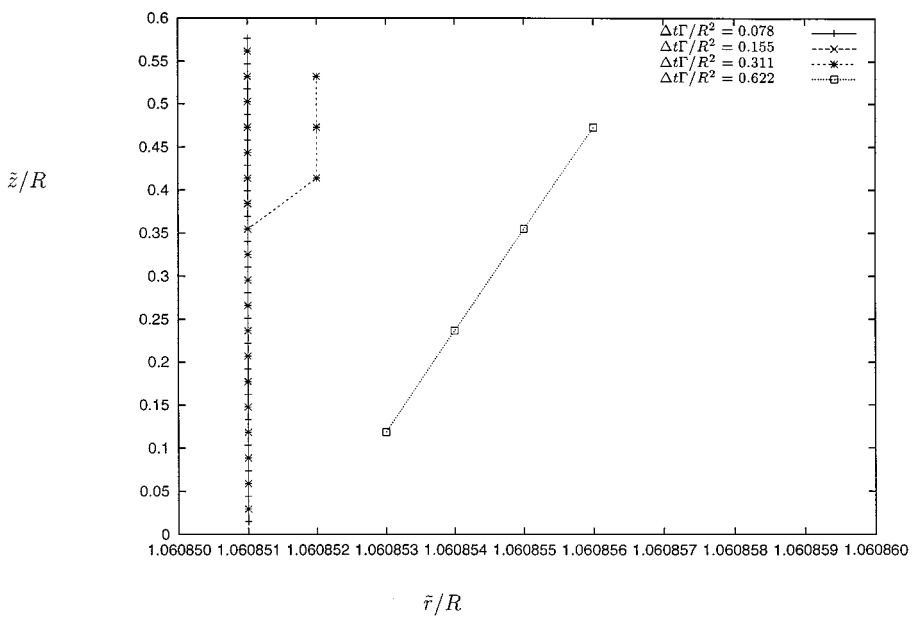

FIG. 10. Trajectory of the vorticity centroid of a Norbury section for different values of the time step $\Delta t\Gamma/R^2$. The initial distribution of the particle is $(r_v, N_p, N_c) = (0.5, 8, 30)$ and $\Delta t\Gamma/R^2$. $\delta/R = 0.03$ and $\varepsilon_0/R = 0.022$.

5.2. *A Pure Diffusion Problem*

In order to check the validity of the diffusion algorithm alone, the following 1D problem has been solved:

$$\frac{\partial \omega}{\partial t} = \nu \left(\frac{\partial^2 \omega}{\partial r^2} - \frac{\omega}{r^2} + \frac{1}{r} \frac{\partial \omega}{\partial r} \right). \tag{61}$$

The particles are characterized by two parameters only: their location r_i and their circulation Γ_i. Using the strength exchange model of Subsection 3.2 leads to the discrete problem

$$\begin{aligned} \Gamma_i(t+\Delta t) = \Gamma_i(t) \left(1 - \exp\left(-\frac{r_i^2}{4\Delta t \nu} \right) \right) + \sum_{j \neq i} (r_j \Gamma_j \mathcal{S}_i - r_i \Gamma_i \mathcal{S}_j) \frac{1}{2\Delta t \nu} \\ \times \exp\left(-\frac{(r_i - r_j)^2}{4\Delta t \nu} \right) \exp\left(-\frac{r_i r_j}{2\Delta t \nu} \right) \mathcal{I}_1 \left(\frac{r_i r_j}{2\Delta t \nu} \right) \\ \frac{dr_i}{dt} = 0. \end{aligned} \tag{62}$$

For the diffusion velocity model of Subsection 3.3, we get

$$\begin{aligned} \frac{d\Gamma_i}{dt} &= -\nu \frac{4 r_i^2 \Gamma_i}{\varepsilon^4} \exp\left(-\frac{r_i^2}{\varepsilon^2} \right) \\ \frac{dr_i}{dt} &= \sum_j u_{\nu r}(r_i, r_j). \end{aligned} \tag{63}$$

The initial conditions are the explicit vorticity distribution derived from Eq. (25) of Subsection 3.2,

$$\omega(r,t) = \frac{\Gamma R}{2t\nu} \exp\left(-\frac{(r-R)^2}{4t\nu} \right) \exp\left(-\frac{rR}{2t\nu} \right) \mathcal{I}_1 \left(\frac{rR}{2t\nu} \right). \tag{64}$$

The corresponding iso-vorticity surfaces are circular cylinders with axis $r = 0$. At radius R, the characteristic diffusion time is the ratio R^2/ν. This ratio vanishes at $r = 0$, leading to an additional difficulty when diffusion close to the axis is strong. Expanding on the time discretization, it is possible for the vortex rings to cross the axis and penetrate the region of negative radius. This difficulty can be overcome by reducing the time step or increasing the order of the integration time scheme. Both procedures lead to an improvement in the accuracy of the particle trajectories.

Figures 11–13 show numerical results for the one-dimensional radial problem using the diffusion velocity model. Figure 11 show the evolution of the vorticity versus radius for two different cutoff numbers and three different instants ($\varepsilon = 0.06$, $\varepsilon = 0.12$). The initial representation (r_i, Γ_i) for the different cases are the same. The comparaison with the analytical results (64) shows that the cutoff $\varepsilon = 0.12$ is too large to represent correctly the vorticity field at $t\nu/R^2 = 0.0225$ (L_2 error $\approx 6\%$), although the diffusion effect is well estimated for larger time (L_2 error $\approx 2\%$). When the cutoff is too small ($\varepsilon = 0.06$), the distance between particles is too large for larger time, resulting in an incorrect vorticity approximation near the axis. For a large range of cutoff ($\varepsilon = 0.03$, $\varepsilon = 0.18$) the relative error estimate between the computed and analytical results has been given for the total circulation and the impulse.

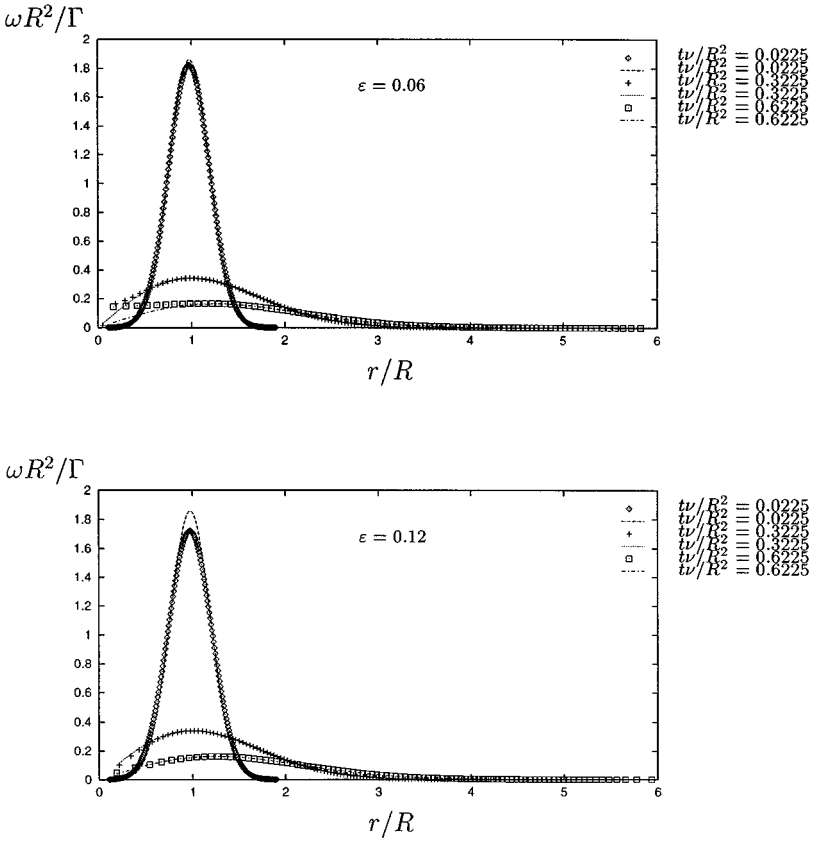

FIG. 11. Numerical results of a pure one-dimensional axisymmetric diffusion. Evolution of vorticity ($\omega R^2/\Gamma$) versus location of vortex particles (r/R) at three different instants in time using the Diffusion Velocity Method. These results are compared to the exact solution (solid line). The numerical parameters are the time step $\Delta t\nu/R^2 = 0.005$ and the cutoff number $\varepsilon/R = 0.06$ (top) and $\varepsilon/R = 0.12$ (bottom). The initial discretization is $(r_v/R, N_c) = (0.9, 90)$. Then the total number of particles is 199.

The L_2 error on the vorticity filed has been also plotted. The cutoff should be evaluated using the mean distance between two neighboring particles at large time. For the axisymmetric case this distance can be very different for particles close to the axis and particles with larger values of r_i. The cutoff $\varepsilon = 0.12$ was selected as a good compromise to estimate correctly the lux of vorticity on the axis ($\Gamma(t)$) and respect the total impulse conservation ($<1\%$) (Fig. 13).

The numerical results using the Strength Exchange Model have been plotted in Figs. 14 and 15. Figure 14 represents the evolution of circulation on each particles compared with the vorticity integrated on the particle ($\Gamma \approx \omega S$). Here the particles are fixed and the initial support of vorticity at $t\nu/R^2 = 0.0225$ extends from $r/R = 0$ to $r/R = 6$: this was found necessary for a large enough computation domain for the larger time ($t\nu/R^2 = 0.5225$). It must be pointed out that for this pure diffusion problem, there is no particle displacement when using the strength exchange model so the time step does not have too much effect on the computed solution (Fig. 15).

Both solutions are in good agreement with the exact solution (Figs. 13 and 16). The impulse is conserved by the strength exchange model 15 whereas a 0.3% error has been obtained with the diffusion velocity model (Fig. 12).

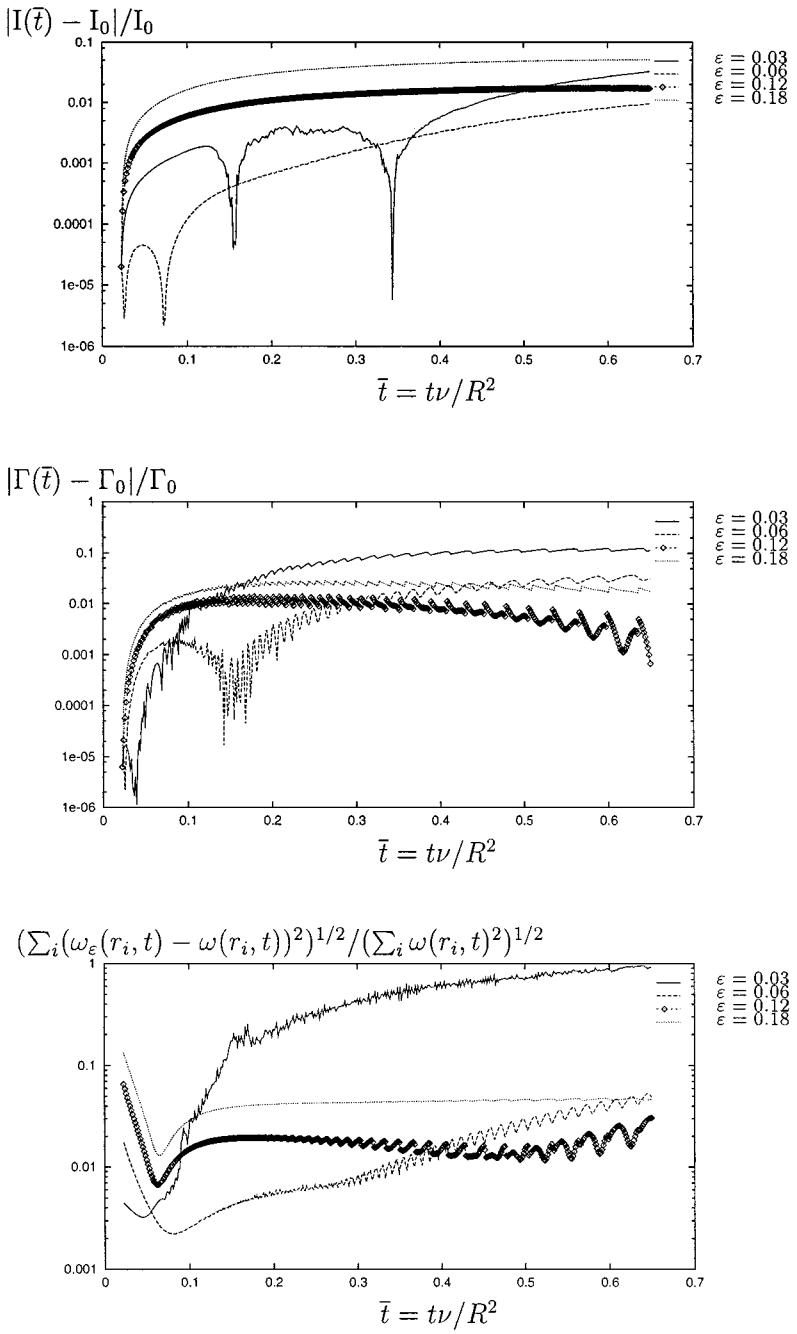

FIG. 12. Error on the impulse (top), the circulation (middle), and the norm L_2 on the vorticity field (bottom) versus time for different cutoff number ε using the Diffusion Velocity Model. The over parameters are the same as in Fig. 11.

In order to confirm that these properties still hold for 2D axisymmetric flows, the pure diffusion of a vortex core has been considered using the diffusion velocity model. The numerical results are plotted in Figs. 17 and 18. The extension of the vorticity domain (Fig. 17) is illustrated by the evolution at three different times of the position of the particles.

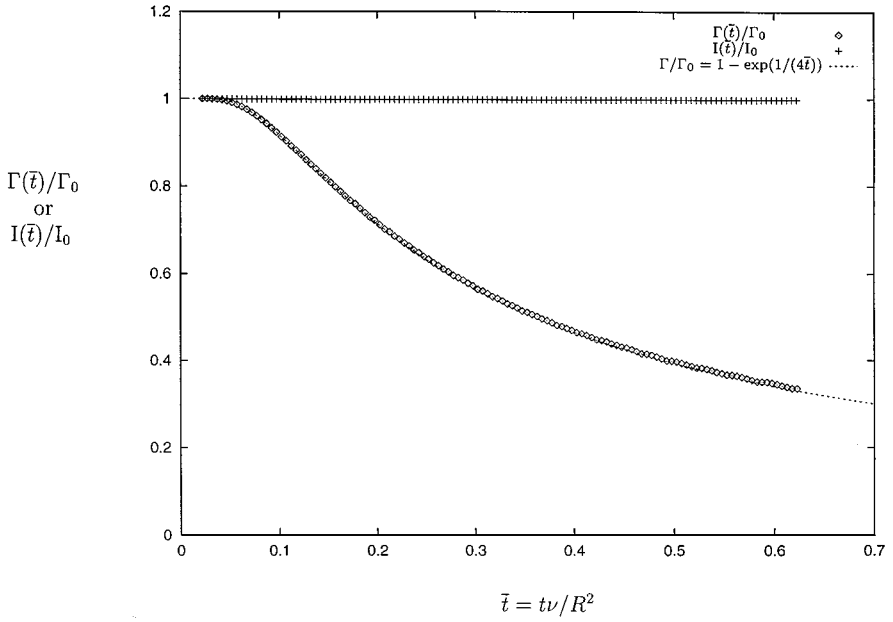

FIG. 13. Numerical results of a pure one-dimensional axisymmetric diffusion using the Diffusion Velocity Model. Evolution of the total circulation ($\Gamma(\bar{t})/\Gamma_0$) and the impulse ($I(\bar{t})/I_0$) versus time ($\bar{t}$). These results are compared with the exact solution. The cutoff number $\varepsilon = 0.12$ and the other parameters are the same as in Fig. 11.

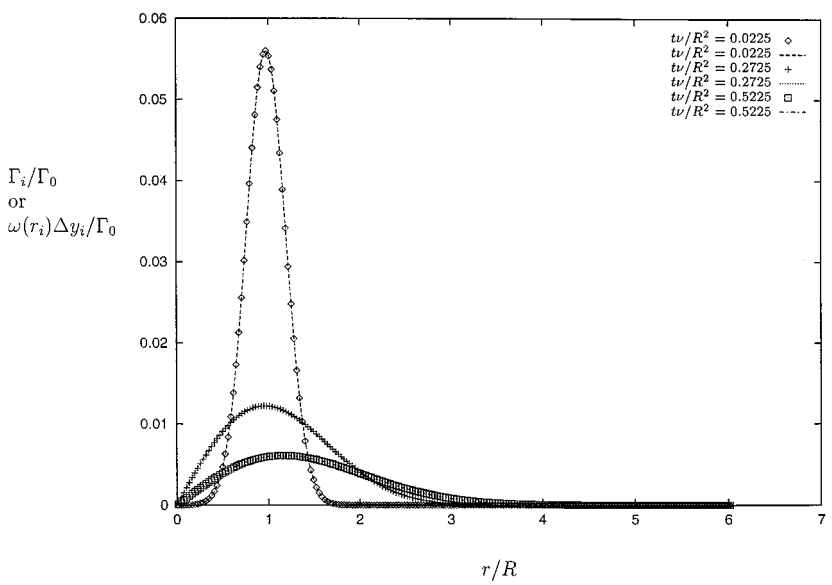

FIG. 14. Numerical results of a pure one-dimensional axisymmetric diffusion. Evolution of circulation on each particle (Γ_i/Γ_0) versus location (r/R) for three different instants in time using the Green's Function Method. The time step is $\Delta t\nu/R^2 = 0.005$ and 199 particles are distributed from $r/R = 0$ to $r/R = 6$. The circulation on each particle is compared with the analytical vorticity integrated on the support of the particle $\approx \omega(r_i)\Delta y_i$.

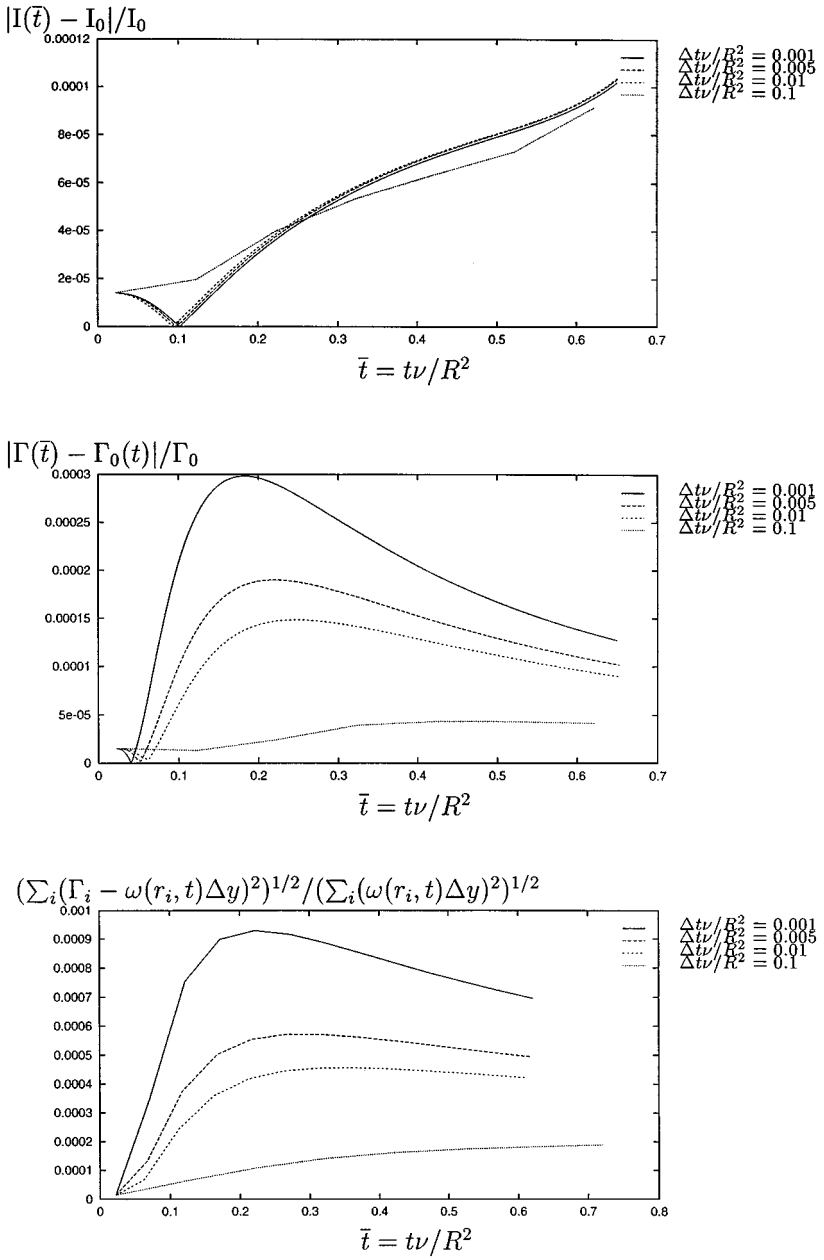

FIG. 15. Error on the impulse (top), the circulation (middle), and the norm L_2 on the *circulation* field (bottom) versus time for a different time step using the Green's Function Method. The over parameters are the same as in Fig. 14.

There is a good agreement with the exact solution. The error for the circulation and the total impulse is arround 1% and the L_2 error on the vorticity field is less than 0.1%.

5.3. *The Viscous Vortex Ring Problem*

For the Navier–Stokes problem solved in this section, only the diffusion velocity model has been computed using the diffusion velocity model. A lot of work has been done with

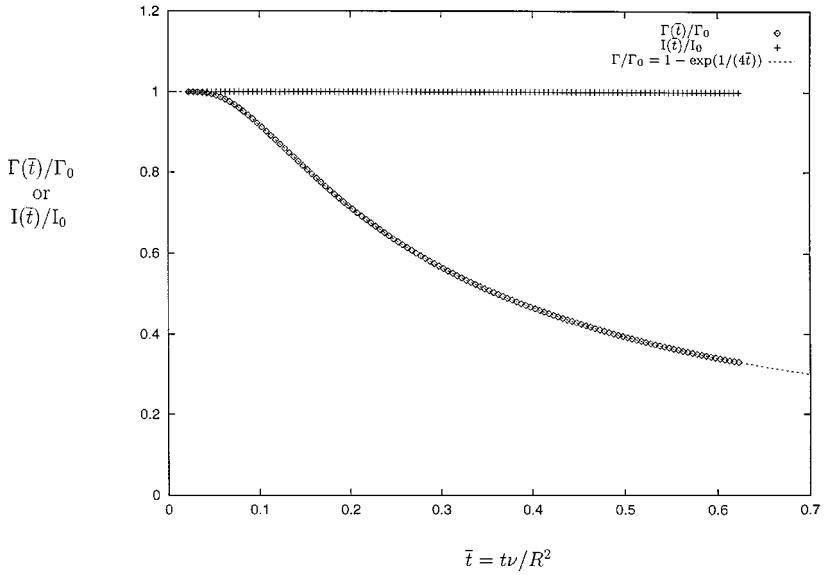

FIG. 16. Numerical results of a pure one-dimensional axisymmetric diffusion using the Green's Function Method. Evolution of the circulation $(\Gamma(\bar{t})/\Gamma_0)$ and the impulse $(I(\bar{t})/I_0)$ versus time $(\bar{t})$. These results are compared to the exact solution.

the vortex ring problem since the Helmholtz 1858 paper. Explicit solutions have been obtained for the steady inviscid case with various core vorticity distribution [10]. The viscous unsteady case has been defined (Tung and Ting [28] and Saffman [25]). Using asymptotic methods on the energy argument, they obtained an explicit formula for the self-induced velocity decay due to vorticity diffusion. For a Gaussian core vorticity distribution (58) and as long as the core radius $\sigma(t) = \sqrt{4\nu t}$ remains small compared to the core radius r_0 this velocity is

$$U_{zc} = \frac{dz_c}{dt} = \frac{\Gamma_0}{4\pi r_0}\left\{\log\left(\frac{8r_0}{\sigma(t)}\right) - 0.558\right\}. \tag{65}$$

The numerical self-induced velocity can still be computed with formula (53). Equation (58) is used to define the initial particles distribution. The vortex core at different time steps is plotted in Fig. 19. The ring self-induced velocity is compared to the asymptotic solution of Saffman [25] in Fig. 20, which shows that the difference between the two predictions is less than 0.7%.

For intermediate Reynolds number ($R_e = \Gamma/\nu$) the convection and diffusion terms in Navier–Stokes equations are of equal magnitude. Figures 21 and 22 show the vorticity field and the position of the particles for $R_e = 500$. This initial condition is obtained at $\bar{t} = t\Gamma/R^2 = 11.15$. Equation (25) has been used to derive the initial distribution of vorticity in the core.

The evolution of the vorticity field with time could be compared with the computations of Stanaway *et al.* [27] which use similar initial conditions. The entrainment and wake formation phase defined by Shariff and Leonard [26] are presented here. According to the "Saffman diffusion process" (pure core spreading) the volume of the core increases with time due to the entrainment of external fluid (Fig. 22). But it's only in the later results

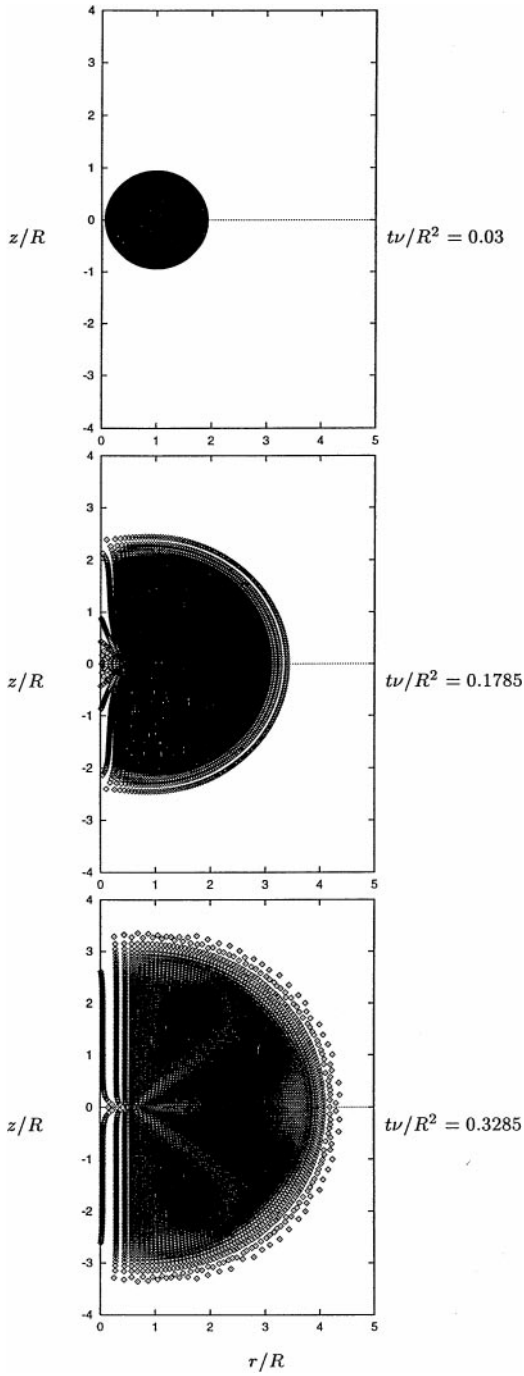

FIG. 17. Numerical results of the pure diffusion of an axisymmetric vortex core. Position of particles at three instants in time. The initial distribution of vorticity is gaussian (Eq. (25)) and the initial condition is obtained at $t\nu/R^2 = 0.03$. $(r_v, N_p, N_c) = (0.9, 4, 80)$ (12971 particles), $\varepsilon = 0.12$, and $\delta t\nu/R^2 = 0.0015$.

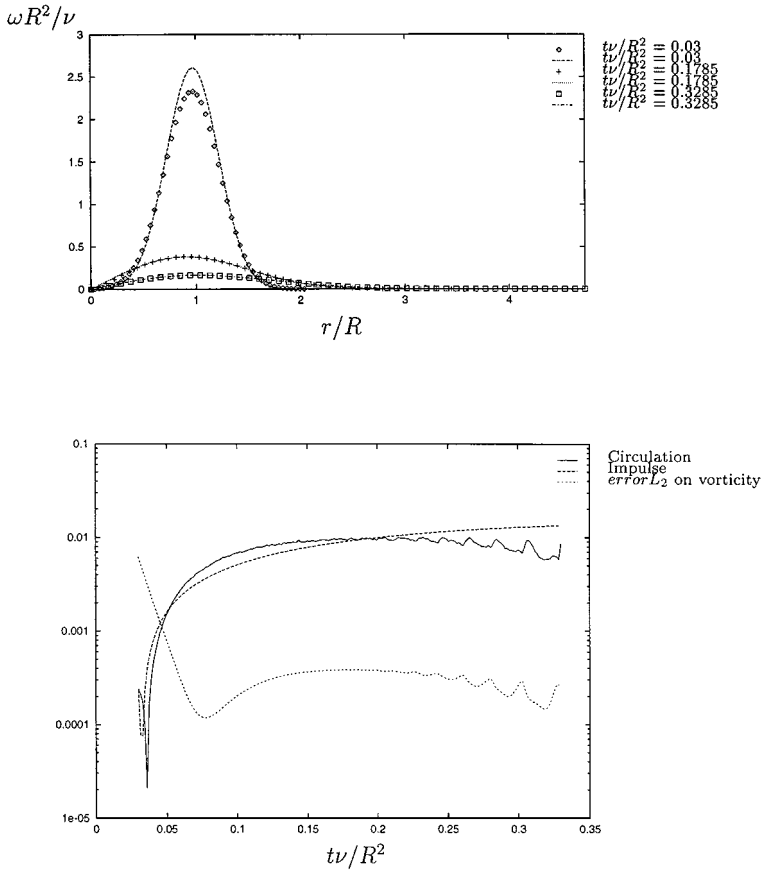

FIG. 18. Vorticty distribution along the r axis for $z = 0$ at different instants in time (top). Error on the impulse, the circulation, and the norm L_2 on the vorticity field versus time using the Diffusion Velocity Model (bottom). The numerical parameters are the same as in Fig. 17.

that the wake formation phase can be observed as well as the formation of a tail (Fig. 21 at $\bar{t} = 21.15$) which decrease in intensity because of the diffusion effects. The formation of the tail implies that vorticity is shed in the wake of the bubble where the intensity is significant. For particles in the tail with small circulation (there is no significant isovalue of vorticity in this region), the fluid convection is not a dominant effect and their motion is mainly governed by diffusion. At this stage it can be expected that dissipation would appear according to Maxworthy's predictions [19], although it has not been taken into account in the present work. In Fig. 23 we present the evolution of circulation and impulse versus time for two different cutoffs: $\varepsilon = 0.12$ and $\varepsilon = 0.06$. In order to ensure the quality of the approximation of ω_ε at any time during the computation, the particle number has been increased up to 12,971. In this case the local relative error on the impulse is lower than 1.5% at the end of the simulation for $\varepsilon = 0.06$ and $\approx$7% for $\varepsilon = 0.12$.

6. CONCLUSION

In this paper, we have proposed an alternative method for the discretization of external axisymmetric flows. The two problems which have been more specifically addressed are

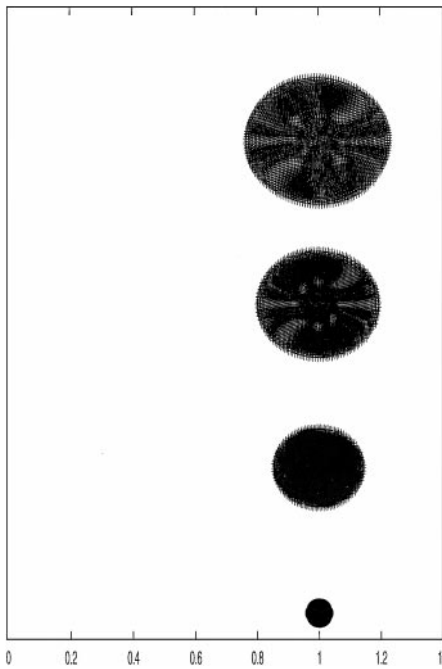

FIG. 19. Location of the vortex particles in the (r, z) plane at different times: $t\nu/R^2 = 0.5\,10^{-4}$, $6.5\,10^{-4}(b)$, $12, 5 \cdot 10^{-4}(c)$, $18.5\,10^{-4}(d)$. $(r_v, N_p, N_c) = (0.04, 4, 40)$, $\delta/R = 0.0025$ and $\varepsilon = 2\delta$, $\Delta t\nu/R^2 = 3\,10^{-5}$, and $\Gamma/\nu = 10$.

the derivation of a so-called deterministic algorithm for diffusion and the axis boundary conditions. Besides this, all the well known qualities of the particle method, namely vorticity conservation and easy modelling of unbounded flows, have been preserved. A particular problem concerning viscous flow representation by integral approximation is that the infinite

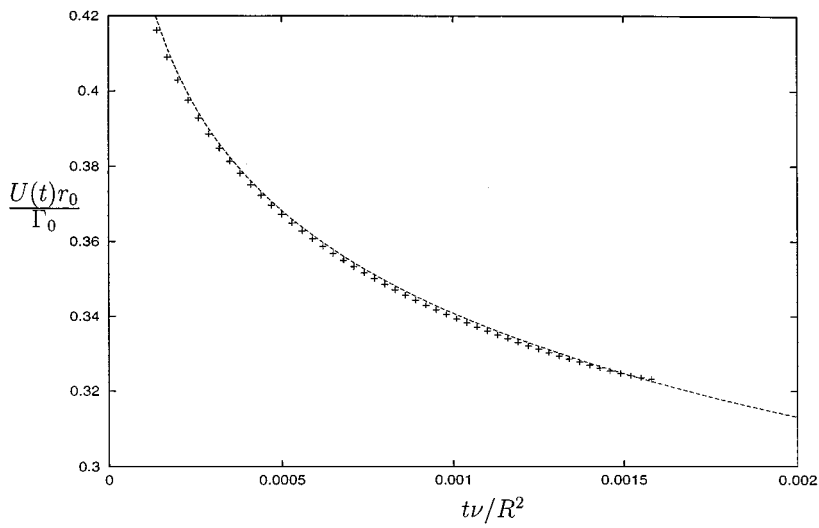

FIG. 20. Evolution of the core self induced velocity of vorticity centroid. The numerical result is compared to the asymptotic solution of Saffman. $(r_v, N_p, N_c) = (0.04, 4, 40)$, $\delta/R = 0.0025$ and $\varepsilon = 2\delta$, $\Delta t\nu/R^2 = 3 \cdot 10^{-5}$, and $\Gamma/\nu = 10$.

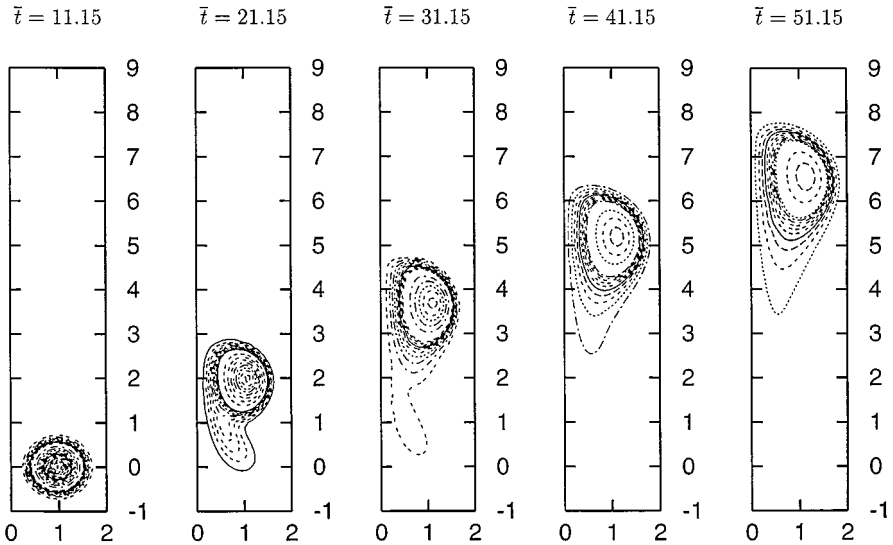

FIG. 21. Vorticity field at several instants in time for $R_e = 500$. The initial condition is obtained at $\bar{t} = 11.15$. $(r_v, N_p, N_c) = (0.7, 4, 50)$, $\delta/R = 0.06$, and $\varepsilon = 2\delta$. The time step is $\Delta t\Gamma/R^2 = 0.1$. The isovalue levels are the same in all plots. The increment step is 0.02 for levels from 0.02 to 0.18 and after the levels are 0.2 to 3.2 with increment step of 0.2.

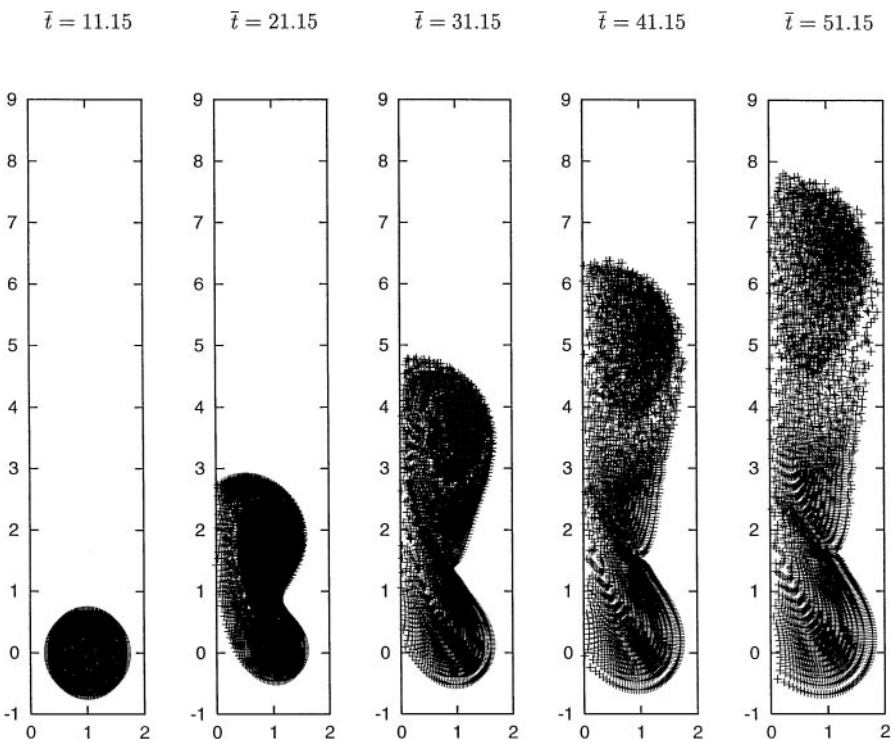

FIG. 22. Evolution of the particles position for $\Gamma/\nu = 500$. The initial conditions are $\bar{t} = 11.15$, $\delta/R = 0.06$, and $\varepsilon = 2\delta$.

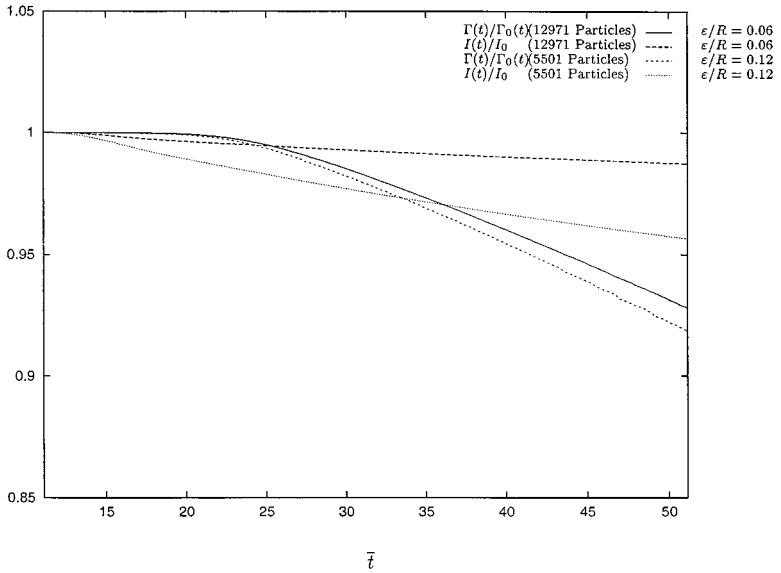

FIG. 23. Evolution of circulation and impulse versus time for two different cutoffs $\varepsilon = 0.06$, $\varepsilon = 0.12$, and $\Gamma/\nu = 500$.

computational domain has to be covered by the particles. The diffusion velocity method like the random vortex method overcomes this difficulty by a constant adaptation of the particles location to the extension of the vorticity support. The main advantage of our method relies in the treatment of the axisymmetric diffusion equations which is resolved in a one step procedure.

Although a lot of interesting problems can be studied within the axisymmetric flow framework, we plan now to complete our method in two directions: the introduction of the azimuthal component of the velocity and the introduction of turbulence models.

APPENDIX

Integral Solution for the Axisymmetric Diffusion Equation

We want to solve the diffusion problem for 3D vorticity,

$$\begin{aligned} \frac{\partial \boldsymbol{\omega}}{\partial t} &= \nu\left(\frac{\partial^2 \boldsymbol{\omega}}{\partial x^2} + \frac{\partial^2 \boldsymbol{\omega}}{\partial y^2} + \frac{\partial^2 \boldsymbol{\omega}}{\partial z^2}\right) \\ \boldsymbol{\omega}(\mathbf{x}, 0) &= \boldsymbol{\omega}_o(\mathbf{x}) \end{aligned} \tag{66}$$

for which an integral solution is

$$\boldsymbol{\omega}(\mathbf{x}, t) = \int_V \boldsymbol{\omega}_o(\mathbf{x}') \frac{1}{(4\pi\nu t)^{3/2}} \exp \frac{(x-x')^2 + (y-y')^2 + (z-z')^2}{4\nu t}\, dx'\, dy'\, dz'. \tag{67}$$

A discrete solution using the particle discretisation can be obtained according to [5],

$$\Omega_i = \sum_j (\Omega_j \mathcal{V}_i - \Omega_i \mathcal{V}_j) \frac{1}{(4\pi\nu t)^{3/2}} \exp \frac{(x_i - x_j)^2 + (y_i - y_j)^2 + (z_i - z_j)^2}{4\nu t} + \mathcal{D}_i, \tag{68}$$

where

$$\begin{aligned}\Omega_i &= \int_{\mathcal{P}_i} \boldsymbol{\omega}(\mathbf{x}, t)\, dx\, dy\, dz \\ \mathcal{V}_i &= \int_{\mathcal{P}_i} dx\, dy\, dz \\ \mathcal{D}_i &= \frac{d}{dt} \int_{R^3} \int_{\mathcal{P}_i} \boldsymbol{\omega}_o(\mathbf{x}') \frac{1}{(4\pi\nu t)^{3/2}} \\ &\quad \times \exp \frac{(x-x')^2 + (y-y')^2 + (z-z')^2}{4\nu t}\, dx'\, dy'\, dz'\, dx\, dy\, dz.\end{aligned} \tag{69}$$

For axisymmetric flows, the vorticity expressed in a cylindrical coordinate system reduces to

$$\boldsymbol{\omega} = \omega e_\theta$$

and satisfies the diffusion equation

$$\frac{\partial \omega}{\partial t} = \nu \left(\frac{\partial^2 \omega}{\partial z^2} + \frac{\partial^2 \omega}{\partial r^2} + \frac{1}{r} \frac{\partial \omega}{\partial r} - \frac{\omega}{r^2} \right).$$

The elementary solution for this equation is

$$\mathcal{G}_{\sqrt{4\nu t}}(r, z, r', z'; t) = \frac{2\pi r'}{(4\pi\nu t)^{3/2}} \exp\left(-\frac{(r-r')^2 + (z-z')^2}{4\nu t} \right) \exp\left(-\frac{r r'}{2\nu t} \right) \mathcal{I}_1\left(-\frac{r r'}{2\nu t} \right).$$

In order to account for the axisymmetric asumption, the computational domain is discretized in a set of torus $\mathcal{T}_i$ with section $\mathcal{S}_i$. The appliction of the previous method leads to

$$\begin{aligned}\Gamma_i(t + \Delta t) &= \int_{\mathcal{S}_i} \sum_j \int_{\mathcal{S}_j} \omega(r', z'; t) \mathcal{G}_{\sqrt{4\nu t}}(r, z, r', z'; t)\, dr'\, dz' \\ &\quad - \int_{\mathcal{S}_i} \sum_j \int_{\mathcal{S}_j} \omega(r, z; t) \mathcal{G}_{\sqrt{4\nu t}}(r, z, r', z'; t)\, dr'\, dz' \\ &\quad - \int_t^{t+\Delta t} \frac{d}{dt} \int_{R \times R^+} \tilde{\omega}(r', z'; \tau)\, dr'\, dz'\, d\tau,\end{aligned} \tag{70}$$

where $\tilde{\omega}$ is the part of the vorticity field corresponding to the diffusion of the vorticity initially in $\mathcal{S}_i$:

$$\tilde{\omega}(r, z; t) = \int_{\mathcal{S}_i} \omega(r', z'; \Delta t) \mathcal{G}_{\sqrt{4\nu t}}(r, z, r', z'; t)\, dr'\, dz'.$$

The last term can be rewritten

$$\int_t^{t+\Delta t} \frac{d}{dt} \int_{R \times R^+} \tilde{\omega}(r', z'; \tau)\, dr'\, dz'\, d\tau = \int_t^{t+\Delta t} -\nu \int_{-\infty}^{\infty} \left(\frac{\partial \tilde{\omega}}{\partial r} + \frac{\tilde{\omega}}{r} \right) \Big|_{r=0} dz\, d\tau.$$

Using the particles approximation and the expression for $\tilde{\omega}$ yields

$$
\begin{aligned}
&\Gamma_i(t+\Delta t)\\
&\quad=\sum_j \Gamma_j \mathcal{S}_i \mathcal{G}_{\sqrt{4\nu\Delta t}}(r_i, z_i, r_j, z_j; \Delta t) - \Gamma_i \mathcal{S}_j \mathcal{G}_{\sqrt{4\nu\Delta t}}(r_j, z_j, r_i, z_i; \Delta t)\\
&\qquad+\int_t^{t+\Delta t} \nu\Gamma_i(t) \int_{-\infty}^{\infty} \frac{\partial}{\partial r}\mathcal{G}_{\sqrt{4\nu\Delta t}}(r_i, z_i, r, z; \tau) + \frac{1}{r}\mathcal{G}_{\sqrt{4\nu\Delta t}}(r_i, z_i, r, z; \tau)\, dz \Big|_{r=0} d\tau\\
&\quad=\Gamma_i(t)\left(1-\exp\left(-\frac{r_i^2}{4\Delta t\nu}\right)\right)+\sum_{j\neq i}(r_j\Gamma_j(t)\mathcal{S}_i - r_i\Gamma_i(t)\mathcal{S}_j)\frac{2\pi}{(4\pi\Delta t\nu)^{3/2}}\\
&\qquad\times\exp\left(-\frac{(r_i-r_j)^2+(z_i-z_j)^2}{4\Delta t\nu}\right)\exp\left(-\frac{r_i r_j}{2\Delta t\nu}\right)\mathcal{I}_1\left(\frac{r_i r_j}{2\Delta t\nu}\right).
\end{aligned}
$$

REFERENCES

1. W. T. Ashurst and E. Meiburg, Three dimensional shear layer via vortex dynamics, *J. Fluid Mech.* **189**, 87 (1988).
2. J. T. Beale and A. Majda, Vortex method. II. Higher order accuracy in two and three dimensions, *Math. Comput.* **39**, 29 (1982).
3. H. S. Carslaw and J. C. Jaeger, *Conduction of Heat in Solids*, 2nd ed. (Oxford Science Publications, 1959).
4. J. Chaumette, *Etude aérodynamique de l'écoulement dans les cavités avec injection pariétale*, Thèse, Note Technique, ONERA 1976-9, Université Paris 6.
5. J. P. Choquin and S. Huberson, Particle Simulation of viscous flow, *Comput. & Fluids* **17**, 397 (1989).
6. A. J. Chorin, Numerical study of slightly viscous flow, *J. Fluid Mech.* **57**, 785 (1973).
7. G. H. Cottet and S. Mas-Gallic, A particle method to solve the Navier–Stokes system, *Numer. Math.* **57**, 805 (1989).
8. G. H. Cottet, On the convergence of vortex methods in two and three dimensions, *Ann. Inst. H. Poincaré* **5**, 227 (1988).
9. P. Degond and S. Mas-Gallic, The weighted particle method for convection-diffusion equations. Part. 1. The case of an isotropic viscosity, *Math. Comput.* **53**, 485 (1990).
10. L. E. Fraenkel, On steady vortex rings of small cross section in an ideal fluid, *Proc. R. Soc. London A* **316**, 29 (1970).
11. J. Fronteau and P. Combis, A lie-admissible method of integration of Fokker–Plank equations with non-linear coefficients (exact and numerical solution), *Hadronic J.* **7**, 911 (1984).
12. P. Genoux, *Etude asymptotique du mouvement et des oscillations d'un tore de vapeur Modélisation d'un jet cavitant oscillant*, Thèse, Université Paris 6, 1988.
13. L. F. Martins and A. F. Ghoniem, Simulation of the nonreacting flow in a Bluff–Body burner; effect of the diameter ratio, *J. Fluids Eng.* **115**, 474 (1993).
14. O. M. Knio and A. Ghoniem, Numerical study of a three-dimensional vortex method, *J. Comput. Phys.* **86**, 75 (1990).
15. H. Lamb, *Hydrodynamics* (Dover, New York, 1932).
16. N. N. Lebedev, *Special Functions and Their Applications* (Dover, New York, 1965).
17. A. Leonard, Computing three-dimensional incompressible flows with vortex elements, *Annu. Rev. Fluid Mech.* **17**, 523 (1985).
18. J. E. Martin and E. Meiburg, Numerical investigation of three dimensionally evolving jets subject to axisymmetric and azimuthal pertubations, *J. Fluid Mech.* **230**, 271 (1991).
19. T. Maxworthy, The structure and stability of vortex rings, *J. Fluid Mech.* **51**, 15 (1972).

20. M. Nitsche and R. Krasny, A numerical study of vortex ring formation at the edge of circular tube, *J. Fluid Mech.* **276**, 139 (1994).
21. M. Nitsche, *Axisymmetric Vortex Sheet Roll-Up*, Ph.D. Thesis, University of Michigan, 1992.
22. J. Norbury, A family of steady vortex rings, *J. Fluid Mech.* **57**, 417 (1973).
23. P. A. Raviart, *Méthodes particulaires*, Lectures Notes, Ecole d'été d'analyse numérique, Centre d'étude du Bréau-sans-nappes, France, 1987.
24. E. Rivoalen, S. Huberson, and F. Hauville, Simulation numérique des équations de Navier Stokes 3D par une méthode particulaire, *C. R. Acad. Sci. Paris Sér. II* **324**, 543 (1997).
25. P. G. Saffman, The velocity of viscous vortex rings, *Stud. Appl. Math.* **49**, 371 (1970).
26. K. Shariff and A. Leonard, Vortex rings, *Annu. Rev. Fluid Mech.* **24**, 235 (1992).
27. S. Stanaway, B. J. Cantwell, and P. R. Spalart, *Navier–Stokes Simulation of Axisymmetric Vortex Rings*, AIAA Paper, No. 88-0318, 1988.
28. C. Tung and L. Ting, Motion and decay of a vortex ring, *Phys. Fluids* **10**, 901 (1967).